Asian Research Journal of Mathematics

8(1): 1-13, 2018; Article no.ARJOM.38684
ISSN: 2456-477X

Numerical Study of Dependent Viscosity and Dependent Thermal Conductivity on a Natural Convection Flow over a Sphere in Presence of Heat Generation

Md. M. Alam[1], Rina Begum[1], Raihanul Haque[1] and M. M. Parvez[1*]

[1]Department of Mathematics, Dhaka University of Engineering and Technology, Gazipur, Bangladesh.

Authors' contributions

This work was carried out in collaboration between all authors. Author MMA designed the study, performed the statistical analysis, wrote the protocol and wrote the first draft of the manuscript. Authors RB and MMP managed the analyses of the study. Authors RH and MMP managed the literature searches. All authors read and approved the final manuscript.

Article Information

DOI: 10.9734/ARJOM/2018/38684
Editor(s):
(1) Cenap Ozel, Mathematics, King Abdulaziz University (KAU), Saudi Arabia and Dokuz Eylul University, Turkey.
Reviewers:
(1) Jagdish Prakash, University of Botswana, Botswana.
(2) José Martínez Reyes, University of the Ciénega of Michoacán State, México.
(3) A. O. Oluwajobi, Obafemi Awolowo University, Nigeria.
Complete Peer review History: http://www.sciencedomain.org/review-history/22681

Original Research Article

Received: 7th December 2017
Accepted: 3rd January 2018
Published: 10th January 2018

Abstract

The objective of this research is to investigate the conjugate effects of dependent viscosity and dependent thermal conductivity on natural convection flow of an electrically conducting fluid over an isothermal sphere with heat generation. Viscosity is considered to be variation and also thermal conductivity is taken as a linear function of temperature. The governing equations are solved numerically by numerical solution strategy as per requirement and suitability. Solution method such as finite difference method with keller box scheme has been employed. The computational findings for dimensionless velocity profiles, temperature profiles, local skin friction coefficient and local heat transfer coefficient are displayed graphically.

Keywords: Heat generation; dependent viscosity; dependent thermal conductivity; Prandtl's number.

**Corresponding author: E-mail: mmparvez@duet.ac.bd;*

1 Introduction

Natural convection takes place while the density difference occurred due to the temperature variations in the fluid. Natural convection has a great deal in attention to the researchers because of its presence both in nature and engineering applications. In addition the problem of natural convection flow over sphere has much interest to the scientists and researchers for their various applications. In engineering applications convection is commonly visualized in the formulation of microstructures during the cooling of molten metal and flowing of fluid around shrouded heat dissipation fins, solar ponds, petroleum reservoir, nuclear energy, fire engineering etc. A very common industrial application of natural convection is free air cooling without the aid of fans. Moreover, viscosity is a measure of internal fluid friction due to the resistance of fluid flow. On the other hand, thermal conductivity is a measure of the ability of heat transfer. Considering, the importance of viscous dissipation and thermal conductivity a lot of research works have been accomplished by many researchers. Alam et al. [1] investigated the viscous dissipation effects on MHD natural convection flow over a sphere in the presence of heat generation. The effect of viscous dissipation on natural convection flow along a sphere with heat generation is considered by Akter, S. et al. [2]. Miraj et al. [3] discussed the conjugate effects of radiation and viscous dissipation on natural convection flow over a sphere with pressure work. Molla M.M. et al. [4] have been investigated the effects of temperature dependent viscosity on MHD natural convection flow from an isothermal sphere. The effects of temperature dependent thermal conductivity on MHD free convection flow alone a vertical flat plate with heat generation and Joule heating have been examined by Islam et al. [5]. Nasrin R., et al. [6] have investigated the combined effects of viscous dissipation and temperature dependent thermal conductivity on magneto hydrodynamic (MHD) free convection flow with conduction and joule heating along a vertical flat plate. Gitima [7] presented analysis of the effect of variable viscosity and thermal conductivity in micro polar fluid for a porous channel in presence of magnetic field. Nasrin R. et al. [8], have been investigated MHD free convection flow along a vertical flat plate with thermal conductivity and viscosity depending on temperature. Nabil Eldabe T.M. et al. [9] analyzed the effects of temperature dependent viscosity and viscous dissipation on MHD convection flow from an isothermal horizontal circular cylinder in the presence of stress work and heat generation. Safiqul Islam K. M. et al. [10], have been discussed the effects of temperature dependent thermal conductivity on natural convection flow along a vertical flat plate with heat generation. Molla et al. [11] analyzed the effect of temperature dependent viscosity on MHD natural convection flow from an isothermal sphere. Alim M. M., et al. [12], analyzed the heat generation effects on MHD natural convection flow along a vertical wavy surface with variable thermal conductivity. Md. Raihanul Haque et al. [13] analyzed the effects of viscous dissipation on natural convection flow over a sphere with temperature dependent thermal conductivity. In all of the aforementioned studies, the thermal conductivity was mentioned as a constant quantity and temperature dependent thermal conductivity. This physical property may change with the change of temperature and viscosity. To the best of our knowledge effect of dependent viscosity and temperature dependent thermal conductivity on natural convection flow over a sphere in presence of heat generation has not been studied yet. So, the present work demonstrates this issue. The non- dimensional transformed boundary layer equations which govern the flow are solved numerically by using finite difference method together with keller-box [14] method. Numerical calculations were carried out for different values of the various non-dimensional quantities and then presented in figures.

2 Formulation of the Problem

We consider a steady two-dimensional natural convection boundary layer flow of an electrically conducting and viscous incompressible fluid over a sphere of radius a. The surface temperature of the sphere is assumed as T_w and T_∞ being the ambient temperature of the fluid. When $T_w > T_\infty$ an upward flow is established along the surface due to free convection and the flow is downward for $T_w < T_\infty$. The mathematical model for the assumed physical problem is prescribed by the following conservation equation of mass, momentum and energy.

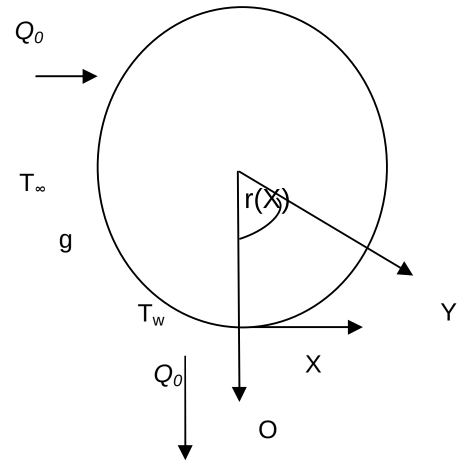

Fig. 1. Physical model and coordinate system

Under these considerations the governing equations are

$$\frac{\partial}{\partial X}(rU)+\frac{\partial}{\partial Y}(rV)=0 \tag{1}$$

$$U\frac{\partial U}{\partial X}+V\frac{\partial U}{\partial Y}=\frac{1}{\rho}\frac{\partial}{\partial Y}\left(\mu\frac{\partial U}{\partial Y}\right)+g\beta(T-T_\infty)\sin\left(\frac{X}{a}\right) \tag{2}$$

$$U\frac{\partial T}{\partial X}+V\frac{\partial T}{\partial Y}=\frac{1}{\rho C_p}\frac{\partial}{\partial Y}\left(k_f\frac{\partial T}{\partial Y}\right)+\frac{Q_0}{\rho c_p}(T-T_\infty) \tag{3}$$

The boundary conditions for the governing equations are

$$\left.\begin{array}{l} U=V=0,\quad T=T_w \quad on \quad Y=0 \\ U\to 0, T\to T_\infty \quad at \quad Y\to\infty \end{array}\right\} \tag{4}$$

$$r(X)=a\ \sin\left(\frac{X}{a}\right) \tag{5}$$

where the radius of sphere is a, r is the radial distance from the symmetrical axis to the surface of the sphere, $k(T)$ is the thermal conductivity of the fluid depending on the fluid temperature *T*. Here we will consider $\mu=\frac{\mu_\infty}{1+\alpha(T-T_\infty)}$ is the dependent viscosity where $\alpha=\frac{1}{\mu_f}\left(\frac{\delta\mu}{\delta T}\right)_f$. We also consider the form of the temperature dependent thermal conductivity which is proposed by Charraudeau [15] as follows:

$k = k_{\infty}\left(1+\gamma^{*}(T-T_{\infty})\right)$, where k_{∞} is the thermal conductivity of the ambient fluid and $\gamma^{*} = \frac{1}{k_f}\left(\frac{\partial k}{\partial T}\right)_f = \frac{\gamma}{(T_w - T_{\infty})}; \gamma = \frac{1}{k_f}\left(\frac{\partial k}{\partial T}\right)(T_w - T_{\infty})$ where γ^{*} is a constant .Equation (3) can be reduced into the following form

$$U\frac{\partial T}{\partial X} + V\frac{\partial T}{\partial Y} = \frac{1}{\rho C_p}\left(\frac{\partial k_f}{\partial Y}\frac{\partial T}{\partial Y} + k\frac{\partial^2 T}{\partial Y^2}\right) + \frac{Q_0}{\rho c_p}\left(T - T_{\infty}\right) \tag{6}$$

3 Transform of the Govern Equations

The above equations are non-dimensional as usual manner by the following substitutions:

$$\xi = \frac{\mathrm{X}}{a}, \eta = \mathrm{Gr}^{1/4}\frac{\mathrm{Y}}{a}, \mathrm{u} = \frac{U}{u_0} = \frac{\mathrm{a}}{\nu}\mathrm{Gr}^{-1/2}\,\mathrm{U}, v = \frac{\mathrm{a}}{\nu}\mathrm{Gr}^{-1/4}V,$$
$$\theta = \frac{\mathrm{T}-\mathrm{T}_{\infty}}{\mathrm{T}_{\mathrm{w}}-\mathrm{T}_{\infty}}, \theta_w = \frac{\mathrm{T}_{\mathrm{w}}}{\mathrm{T}_{\infty}}, T = T_{\infty} + \theta\left(T_w - T_{\infty}\right) \tag{7}$$

where, $u_0 = \frac{\upsilon}{a}Gr^{1/2}$ is the characteristic velocity of the fluids. Here we will consider

$$Q = \frac{a^2 Q_0}{c_p \mu Gr^{\frac{1}{2}}}, \beta = -\frac{1}{\rho}\left(\frac{\delta\rho}{\delta T_f}\right)_p, \; Gr = \frac{g\beta a^3}{\upsilon^2}\left(T - T_{\infty}\right),$$

$$\varepsilon = \frac{1}{\mu_f}\left(\frac{\delta\mu}{\delta T}\right)_f \left(T - T_{\infty}\right), \frac{\mu}{\mu_{\infty}} = \frac{1}{1+\varepsilon\theta}$$

Using the above transformations into equations (1) to (3), we have

$$\therefore \frac{\delta}{\delta\xi}(ru) + \frac{\delta}{\delta\eta}(rv) = 0 \tag{8}$$

$$u\frac{\partial u}{\partial\xi} + v\frac{\partial u}{\partial\eta} = \frac{-\varepsilon}{(1+\varepsilon\theta)^2}\frac{\partial u}{\partial\eta}\frac{\partial\theta}{\partial\eta} + \frac{1}{1+\varepsilon\theta}\frac{\partial^2 u}{\partial\eta^2} + \theta\sin\xi \tag{9}$$

$$u\frac{\partial\theta}{\partial\xi} + \upsilon\frac{\partial\theta}{\partial\eta} = \frac{1}{Pr}(1+\gamma\theta)\frac{\partial^2\theta}{\partial\eta^2} + \frac{1}{Pr}\gamma\left(\frac{\partial\theta}{\partial\eta}\right)^2 + Q\theta \tag{10}$$

The boundary conditions associated with (9) to (10) becomes

$$\left.\begin{array}{l} u = v = 0, \quad \theta = 1 \quad at\ \xi = 0,\ for\ any\ \eta \\ u = v = 0, \quad \theta = 1 \quad at\ \eta = 0, \xi > 0 \\ u \to 0, \quad \theta \to 0\ \ as\ \eta \to \infty,\ \ \xi > 0 \end{array}\right\} \tag{11}$$

Here, $Gr = g\beta(T_w - T_\infty)a^3/\nu^2$ is the Grashof number and θ is the non-dimensional temperature function, $\Pr = \frac{\mu C_p}{k_\infty}$ is the Prandtl's number, $\gamma = \frac{1}{k_f}\left(\frac{\partial k}{\partial T}\right)(T_w - T_\infty)$ is the thermal conductivity variation parameter and $\varepsilon = \frac{1}{\mu_f}\left(\frac{\delta\mu}{\delta T}\right)_f (T - T_\infty)$ is the dependent viscosity parameter. To solve equations (9) and (10) subject to the boundary conditions (11), we assume the following variables u and v where $\psi = \xi\ r(\xi)\ f(\xi,\eta)$ and $\psi(\xi,\eta)$ is a non-dimensional stream function which is related to the velocity components in the usual way as

$$u = \frac{1}{r}\frac{\partial\psi}{\partial\eta} \ \text{ and } \ v = -\frac{1}{\mathrm{r}}\frac{\partial\psi}{\partial\xi}$$

The momentum and energy equations (9) and (10) reduces to

$$\frac{1}{1+\varepsilon\theta}\frac{\delta^3 f}{\delta\eta^3} + \left(1 + \frac{\xi}{\sin\xi}\cos\xi\right) f\,\frac{\delta^2 f}{\delta\eta^2} - \left(\frac{\delta f}{\delta\eta}\right)^2 - \frac{\varepsilon}{(1+\varepsilon\theta)^2}\frac{\delta\theta}{\delta\eta}\frac{\delta^2 f}{\delta\eta^2} + \frac{\theta\sin\xi}{\xi} = \xi\left(\frac{\delta f}{\delta\eta}\frac{\delta^2 f}{\delta\eta\delta\xi} - \frac{\delta f}{\delta\xi}\frac{\delta^2 f}{\delta\eta^2}\right) \tag{12}$$

$$\frac{1}{pr}(1+\gamma\theta)\frac{\delta^2\theta}{\delta\eta^2} + \frac{1}{pr}\gamma\left(\frac{\delta\theta}{\delta\eta}\right)^2 + \left(1 + \frac{\xi}{\sin\xi}\cos\xi\right) f\,\frac{\delta\theta}{\delta\eta} + Q\theta = \xi\left(\frac{\delta f}{\delta\eta}\frac{\delta\theta}{\delta\xi} - \frac{\delta f}{\delta\xi}\frac{\delta\theta}{\delta\eta}\right) \tag{13}$$

The corresponding boundary conditions are

$$\left.\begin{array}{l} f = \frac{\partial f}{\partial\eta} = 0, \quad \theta = 1\ at\ \ \eta = 0 \qquad for\ \ any\ \ \eta \\ f = \frac{\partial f}{\partial\eta} = 0, \quad \theta = 1\ at\ \ \eta = 0, \xi > 0 \\ \frac{\partial f}{\partial\eta} \to 0, \theta \to 0\ \ as\ \ \eta \to \infty, \xi > 0 \end{array}\right\} \tag{14}$$

In practical application, the physical quantities of principal interest are the heat transfer and the skin- friction coefficient, which can be written in non- dimensional form as

$$Nu_\xi = \frac{aGr^{-1/4}}{k\left(T_w - T_\infty\right)} q_w \text{ and } Cf_\xi = \frac{Gr^{-3/4} a^2}{\mu \nu} \tau_w \tag{15}$$

where $q_w = -k_f \left(\frac{\partial T}{\partial Y}\right)_{Y=0}$ and $\tau_w = \mu \left(\frac{\partial U}{\partial Y}\right)_{Y=0}$, k_f being the thermal conductivity of the fluid. Using the new variables (7), we have the simplified form of the heat transfer and the skin- friction coefficient as

$$Nu_\xi = -\left(\frac{\partial \theta}{\partial \eta}\right)_{\eta=0} \text{ and } Cf_\xi = \xi \left(\frac{\partial^2 f}{\partial \eta^2}\right)_{\eta=0} \tag{16}$$

4 Method of Solution

To obtain the solution of the problem, the numerical method used is a finite difference method known as Keller-box [14] method. To begin with, the partial differential equations(12)-(13) are first converted into a system of first order differential equations. Then these equations are expressed in finite difference forms by approximating the functions and their derivatives in terms of the centered differences and two point averages using only values at the corner of the box (or mesh rectangle). Denoting the mesh points in the (ξ, η)-plane by ξ_i and η_j where i = 1, 2, . . . , M and j= 1, 2, . . . , N, central difference approximations are made, such that those equations involving ξ explicitly are centered at $(\xi_{i-1/2}, \eta_{j-1/2})$ and the remainder at $(\xi_i, \eta_{j-1/2})$, where $\eta_{j-1/2} = \frac{1}{2}(\eta_j + \eta_{j-1})$ etc. Grid dependency has been tested and solutions are obtained with grid of optimum dimensions 182×200 in the (ξ, η) domain and non-uniform mesh size is employed to produce results of high accuracy near the coordinate $\xi = 0,\ \eta = 0.$ The central difference approximations reduces the system of first order differential equations to a set of non-linear difference equations for the unknown at ξ_i in terms of their values at ξ_{i-1}. The resulting set of nonlinear difference equations are solved by using the Newton's quasi-linearization method taking as the initial iteration of the converged solution at $\xi = \xi_{i-1}$.Now the initial process at $\xi = 0$, we first provide guess profiles for all five variables and use the keller box method to solve the governing ordinary differential equations. Having obtained the lower stagnation point solution, it is possible to march step by step along the boundary layer. For a given value of ξ, the iterative procedure is stopped when the difference in computing the velocity and the temperature in the next iteration is less than 10^{-6}, *i.e.* when $\left|\delta f^i\right| \le 10^{-6}$, where the superscript denotes the iteration number. A uniform grid of 2001 points are used in the ξ-direction with the step size = 0.01 and another non-uniform grid in the η-direction has been incorporated, considering $\eta_i = \sinh\{(j-1)/p\}$ where j=1, 2,…..301 and p=100 to get quick convergence and thus save computational time and memory space. The Jacobian matrix has a block-tridiagonal structure and the difference equations are solved using a Block-matrix version of the Thomas algorithm; further details of the computational procedure have been discussed in the book by Cebecci and Bradshow [16].

5 Results and Discussion

The problem considered here involves a number of parameters on the basis of which a wide range of numerical results have been derived. Of these results, a small section is presented here for brevity. The numerical results of velocity and temperature profiles and also for local skin frictions as well as local heat transfer coefficient are shown in Fig. 2(a) to Fig. 9(b) for various values of parameters entering into the problem.

Fig. 2(a) shows the effects of the velocity profile for different values of the dependent thermal conductivity parameter γ = 0.10, 0.30, 0.50, 0.70, 0.90 while the other controlling parameters Pr = 0.72, Q = 0.30 and ε = 1.50. Corresponding distribution of the temperature profile is shown in Fig. 2(b). From Fig. 2(a), it is seen that if the dependent thermal conductivity parameter γ increases, the velocity of the fluid also increases. On the other hand, it is observed that the temperature profile increases within the boundary layer due to increase of the dependent thermal conductivity parameter γ which is evident from Fig. 2(b).

From Fig. 3(a) and Fig. 3(b), it can also easily be seen that an increase in the dependent thermal conductivity γ leads to increase the local skin friction coefficient Cf_{ξ} and also the local rate of heat transfer coefficient Nu_{ξ} increase with the increase of dependent thermal conductivity while Prandtl's number Pr = 0.72, heat generation parameter Q = 0.30 and dependent viscosity parameter ε = 1.50. Also it is observed that at any position of ξ, the local skin friction coefficient Cf_{ξ} and the local Nusselt number Nu_{ξ} increase as γ increases from 0.00 to 1.2. This phenomenon can easily be understood from the fact that when the dependent thermal conductivity γ increases, the temperature of the fluid rises and the thickness of the velocity boundary layer grows i.e. the thermal boundary layer becomes thinner than the velocity boundary layer. Therefore the skin friction coefficient Cf_{ξ} and the local Nusselt number Nu_{ξ} are increased.

From Fig. 4(a), it may be concluded that the dependent viscosity increases the velocity field in the region $\eta \in [0, 12]$. The changes of velocity profiles in the η direction reveals the typical velocity profile for natural convection boundary layer flow i.e. the velocity is zero at the boundary of wall then it increases and reaches to the peak value as η increases and finally the velocity approaches to zero for the asymptotic value. The maximum values of the velocity are 0.40934, 0.44132, 0.47876, 0.50425, 0.52296 for ε = 0.10, 1.00, 1.50, 2.00, 2.50 respectively and which occurs at η = 1.23788 for first and second maximum values, at η = 1.36929 for third and fourth maximum values and η = 1.43822 for last maximum value. Here we see that the velocity increases by 27.76% as η increases from 0.10 to 2.50. In Fig. 4(b) it is clearly seen that the temperature distribution increases owing to increase of the values of the dependent viscosity parameter ε and maximum is at the wall.

The effect for different values of dependent viscosity parameter ε (= 0.`10, 1.00, 1.50, 2.00, 2.50), the local skin friction coefficient Cf_{ξ} and local rate heat of transfer coefficient Nu_{ξ} are shown in the Fig. 5(a) and Fig. 5(b) while Pr = 0.72, Q = 0.90 and γ = 0.70. Here, it is seen that as the dependent viscosity parameter ε increases both the local skin friction coefficient and local rate of heat transfer coefficient (Nu_{ξ}) increase.

Fig. 6(a) and Fig. 6(b) illustrate the effect of the heat generation parameter Q (= 0.40, 0.70, 0.90, 1.10) with parameters Pr = 0.72, ε = 0.60 and γ = 0.80 on the velocity profile and the temperature profile. From Fig. 6(a), it is revealed that the velocity profile increases with the increase of the heat generation parameter Q that indicates that heat generation parameter accelerates the fluid motion. Small increment is shown from Fig. 6(b) on the temperature profile for increasing values of Q.

Fig. 7(a) and Fig. 7(b) illustrate the variation of local skin friction coefficient $f''(\xi)$ and the rate of local heat transfer Nu_ξ against ξ for different values of heat generation parameter Q (= 0.40, 0.70, 0.90, 1.10) as obtained by solving numerically equations (7.13) and (7.14) where Pr = 0.72, ε = 0.60 and γ = 0.80. It is seen from Fig. 7(a) that the skin friction coefficient Cf_ξ is influenced considerably and increases when the values of heat generation parameter Q increase at different position of ξ with other controlling parameters. Fig. 7(b) indicates that the rate of local of heat transfer Nu_ξ decreases owing to increase in values of heat generation parameter Q with other fixed parameters.

Fig. 8(a) depicts the velocity profile for different values of the Prandtl,s number Pr (= 0.72, 1.00, 1.74, 2.00, 3.00) with parameters Q = 0.70, ε = 0.50 and γ = 0.90. Corresponding distribution of the temperature profile is shown in Fig. 8(b). From Fig. 8(a), it can be seen that if the Prandtl's number increases, the velocity of the fluid decreases. On the other hand, from Fig. 8(b) we observe that the temperature profile also decreases within the boundary layer due to increase of the Prandtl's number Pr.

Fig. 9(a) and Fig. 9(b) illustrate the variation of local skin friction coefficient Cf_ξ and the rate of local heat transfer Nu_ξ against ξ for different Pr (= 0.72, 1.00, 1.74, 2.00, 3.00) with parameters Q = 0.70, ε = 0.50 and γ = 0.90. as obtained by solving numerically equations (7.13) and (7.14). It is seen from figure 9(a) that the skin friction coefficient Cf_ξ is influenced considerably and decreases when the values of Prandtl's number Pr increase at different position of ξ with other controlling parameters. Fig. 7(b) indicates that the rate of local of heat transfer Nu_ξ increases owing to increase in values of Prandtl's number Pr with other fixed parameters.

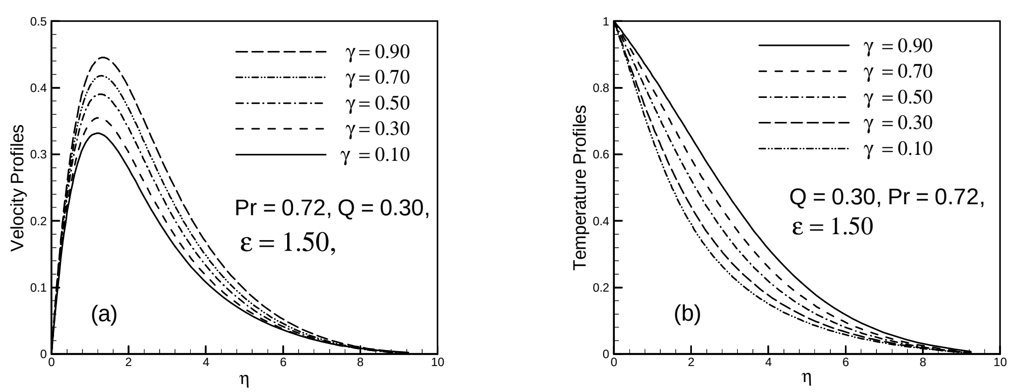

Fig. 2(a) and 2(b). Variation of dimensionless velocity profiles $f'(\eta,\xi)$ and temperature profiles $\theta(\eta,\xi)$ against dimensionless distance η for different values of dependent thermal conductivity parameter γ with Pr = 0.72, ε = 1.50 and Q = 0.30

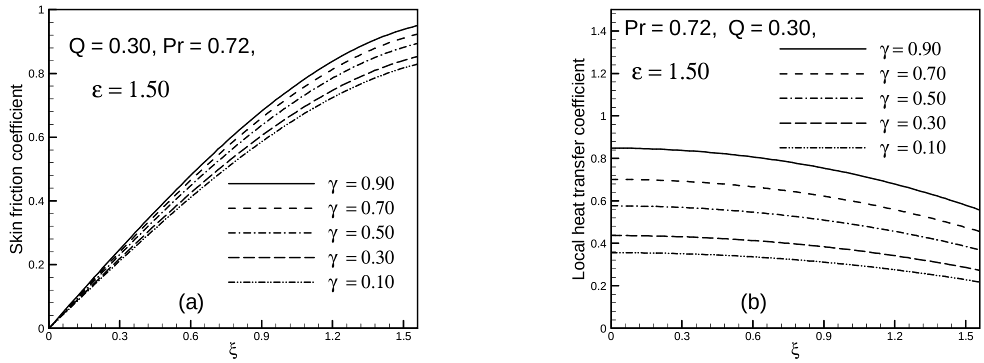

Fig. 3(a) and 3(b). Variation of dimensionless skin friction coefficient $f''(\xi)$ and local Nusselt number, Nu_ξ against dimensionless distance ξ for different values of dependent thermal conductivity parameter γ with *Pr* = 0.72, ε = 1.50 and *Q* = 0.30

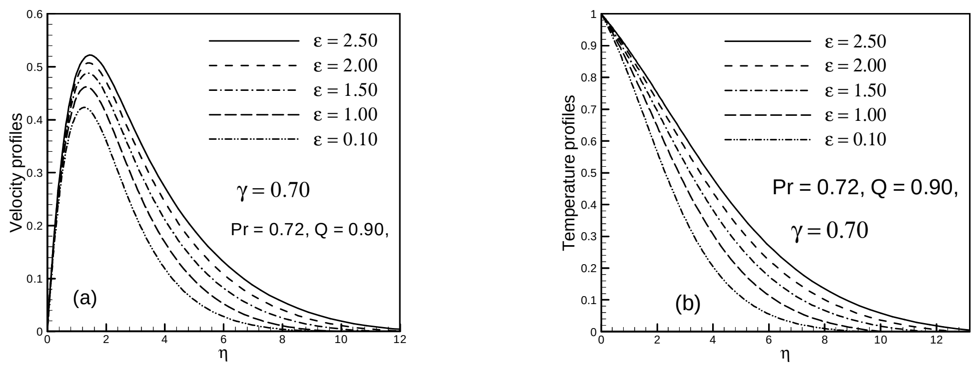

Fig. 4(a) and 4(b). Variation of dimensionless velocity profiles $f'(\eta,\xi)$ and temperature profiles $\theta(\eta,\xi)$ against dimensionless distance η for different values of dependent viscosity parameter ε with *Pr* = 0.72, γ = 0.70 and *Q* = 0.90

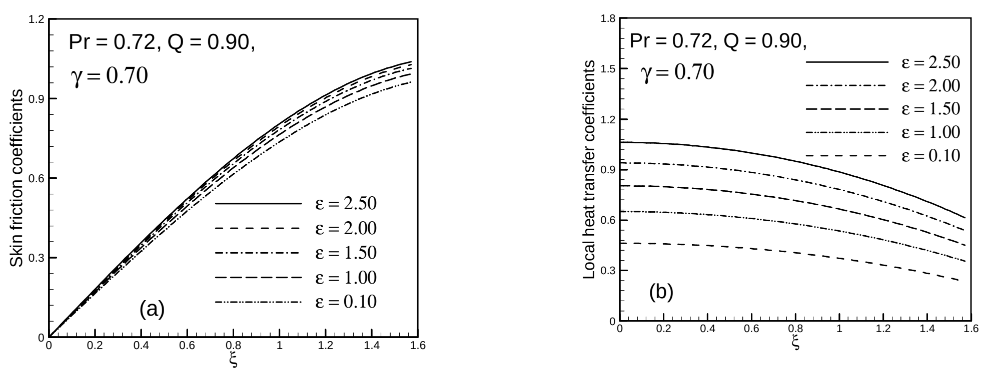

Fig. 5(a) and 5(b). Variation of dimensionless skin friction coefficient $f''(\xi)$ and local Nusselt number, Nu_ξ against dimensionless distance ξ for different values of dependent viscosity parameter ε with *Pr* = 0.72, γ = 0.70 and *Q* = 0.90

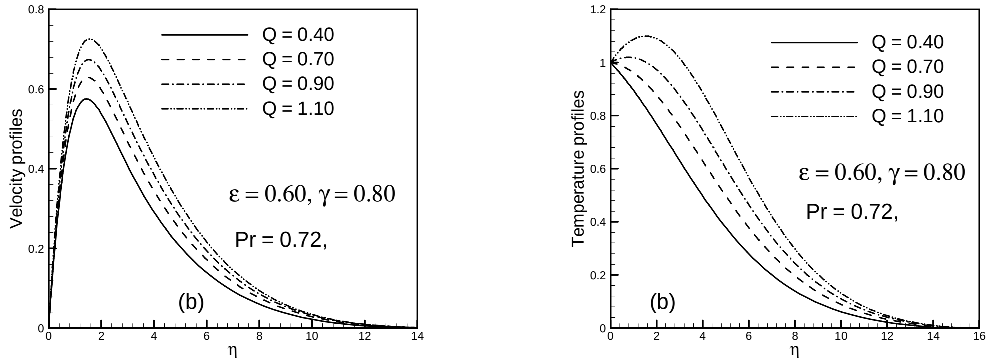

Fig. 6(a) and 6(b). Variation of dimensionless velocity profiles $f'(\eta,\xi)$ and temperature profiles $\theta(\eta,\xi)$ against dimensionless distance η for different values of heat generation parameter *Q* with *Pr* = 0.72, γ = 0.80 and ε = 0.60

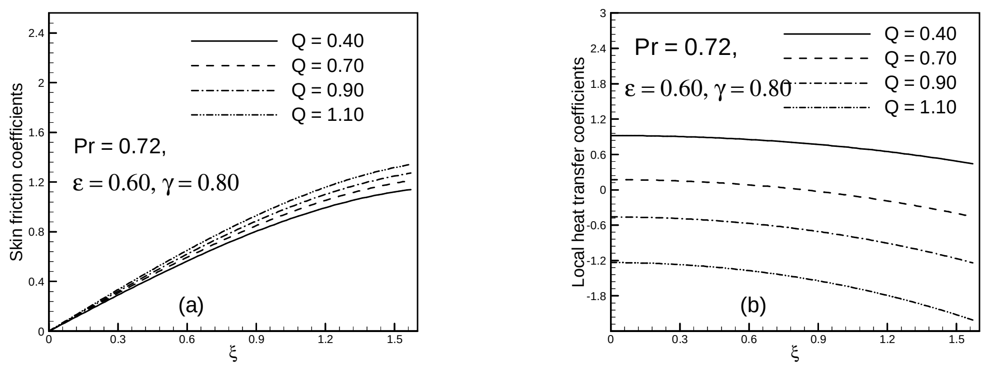

Fig. 7(a) and 7(b). Variation of dimensionless skin friction coefficient Cf_ξ and local Nusselt number, Nu_ξ against dimensionless distance ξ for different values of heat generation parameter *Q* with *Pr* = 0.72, γ = 0.80 and ε = 0.60

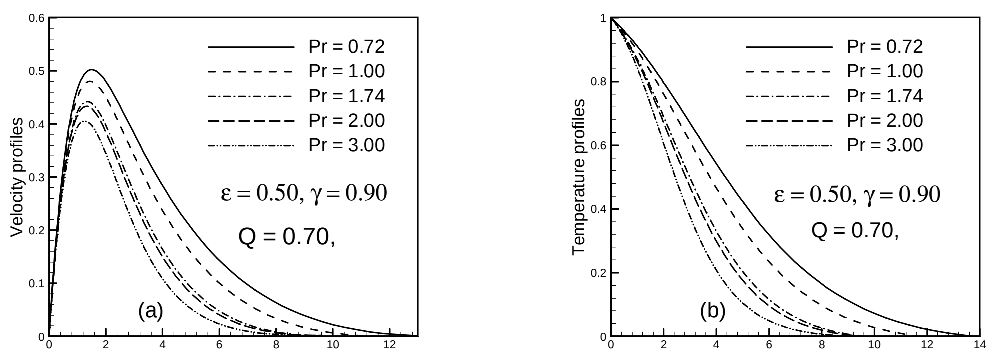

Fig. 8(a) and 8(b). Variation of dimensionless velocity profiles $f'(\eta,\xi)$ and temperature profiles $\theta(\eta,\xi)$ against dimensionless distance η for different values of prandtl's number *Pr* with *Q* = 0.70, γ = 0.90 and ε = 0.50

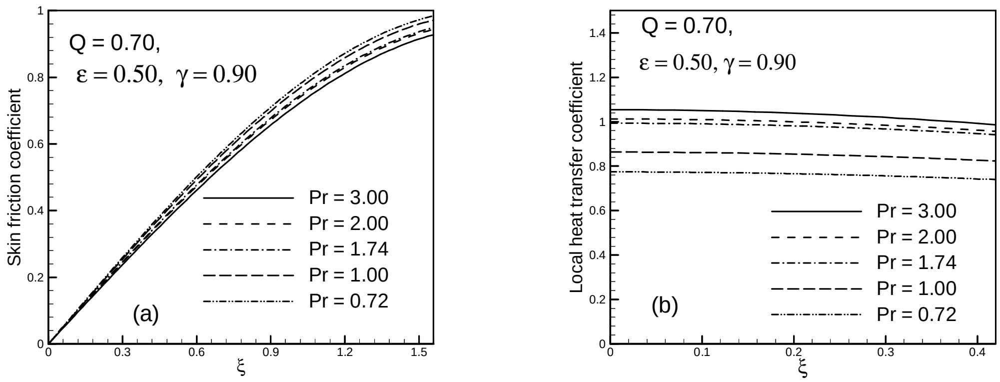

Fig. 9(a) and 9(b). Variation of dimensionless skin friction coefficient Cf_ξ and local Nusselt number, Nu_ξ against dimensionless distance ξ for different values of prandtl's number *Pr* with *Q* = 0.70, γ = 0.90 and ε = 0.50

6 Conclusions

From the present investigation, the following conclusions may be drawn:

- Increase in the values of dependent thermal conductivity parameter γ leads to increase the velocity profile. The temperature profile, the local skin friction coefficient Cf_ξ and also the local rate of heat transfer Nu_ξ increase with the increase of dependent thermal conductivity parameter γ while *Q*=0.30, ε = 1.50 and *Pr* = 0.72.
- The velocity profiles, the temperature profiles, the local skin friction coefficient Cf_ξ and also the local heat transfer coefficient Nu_ξ increase significantly when the values of dependent viscosity parameter ε increase.
- Significant effects of heat generation parameter *Q* on velocity and temperature profiles as well as on local skin friction coefficient and the rate of heat transfer have been found in this investigation but the effect of heat generation parameter *Q* on rate of heat transfer is more significant. An increase in the values of heat generation parameter *Q* leads to both the velocity and the temperature profiles decreases. The local skin friction coefficient Cf_ξ increases at different position of ξ, but the local rate of heat transfer Nu_ξ decreases at different position of ξ for *Pr* =0.72, ε = 0.60 and γ = 0.80.
- Increasing values of Prandtl's number *Pr* leads to decrease the velocity profiles. The temperature profiles, the local skin friction coefficient Cf_ξ but the local rate of heat transfer Nu_ξ increases with the increase of Prandtl's number *Pr* while *Q* = 0.70, ε = 0.50and γ = 0.90.

Competing Interests

Authors have declared that no competing interests exist.

References

[1] Alam MM, Alim MA, Chowdhury MMK. Viscous dissipation effect on MHD natural convection flow over a sphere in the presence of heat generation. Nonlinear Analysis, Modelling and Control. 2007;12(4):447-459.

[2] Aktar S, Mahmuda Binte Mostofa Ruma, Parveen N. Viscous dissipation effects on natural convection flow alone a sphere with heat generation. Global Journal of Science Frontier Research. 2010;10(1).

[3] Miraj M, Alim MA, Shahidul Alam, Karim MR. Conjugate effects of radiation and viscous dissipation on natural convection flow over a sphere with pressure work. International Journal of Science and Technology. 2012;1(3).

[4] Molla MM, Rahman A, Rahman LT. Natural convection flow from an isothermal sphere with temperature dependent thermal conductivity. J. Archit. Marine Eng. 2005;2:53–64.

[5] Safiqul Islam AKM, Alim MA, Sarker ATM, M. R. Effects of temperature dependent thermal conductivity on MHD free convection flow along a vertical flat plate with heat generation and joule heating. The international conference on marine Technology, 11-12 December 2010, BUET, Dhaka, Bangladesh; 2010.

[6] Nasrin R, Alim MA. Combined effects of viscous dissipation and temperature dependent thermal conductivity on magneto hydrodynamic (MHD) free convection flow with conduction and joule heating along a vertical flat plate. Journal of Naval Architecture and Marine Engineering, JNAME. 2009;6(1):30-40.

[7] Gitima Patoway. Effect of variable viscosity and thermal conductivity of micropolar fluid in a porous channel in presence of magnetic field. International Journal for Basic Social Science (IJBSS). 2012;1(3):69-77.
ISBN: 2319-2968.

[8] Nasrin R, Alim MA. MHD free convection flow along a vertical flat plate with thermal conductivity and viscosity depending on temperature. Journal of Naval Architecture and Marine Engineering; 2009.

[9] Nabil T. M. Eldabe, Elsayed M. A. Elbashbeshy, Youssef IK, Ahmed M. Sedki. The effects of temperature dependent viscosity and viscous dissipation on MHD convection flow from an isothermal horizontal circular cylinder in the presence of stress work and heat generation. Journal of European Scientific. 2014;10:36.
ISSN: 1857-7881.

[10] Safiqul Islam KM, Alim MA, Sarker MMA, Khodadad Khan AFM. Effects of temperature dependent thermal conductivity on natural convection flow along a vertical flat plate with heat generation. Journal of Naval Architecture and Marine Engineering; 2012.

[11] Molla MM, Saha SC, Hossain MA. The effect of temperature dependent viscosity on MHD natural convection flow from an isothermal sphere. Journal of Applied Fluid Mechanics. 2012;5(2):25-31.

[12] Md. Abdul Alim, Md. Rezaul Karim, Md. Miraj Akand. Heat generation effects on MHD natural covection flow along a vertical wavy surface with variable thermal conductivity. Journal of Computational Mathematics. 2012;2:42-50.

[13] Md. Raihanul Haque, Alim MM, Alam MM, Alim MA. Effects of viscous dissipation on natural convection flow over a sphere with temperature dependentthermal conductivity. Journal of Computer and Mathematical Sciences. 2014;5:1-12.

[14] Keller HB. Numerical methods in boundary layer theory. Annual Rev. Fluid Mech. 1978;10:417-443.

[15] Charruaudeau J. Influence de gradients de properties physiques en convection force application au cas du tube. International Journal of Heat and Mass Transfer. 1975;18:87-95.

[16] Cebeci T, Brashaw P. Physical and computational aspects of convective heat transfer. Spring, New York; 1984.

© 2018 Alam et al.; This is an Open Access article distributed under the terms of the Creative Commons Attribution License (http://creativecommons.org/licenses/by/4.0), which permits unrestricted use, distribution, and reproduction in any medium, provided the original work is properly cited.

Peer-review history:
The peer review history for this paper can be accessed here (Please copy paste the total link in your browser address bar)
http://sciencedomain.org/review-history/22681